Supplementary Materials for

Spatiotemporal Ferro-Ionic Dynamics in Van der Waals Ferroelectrics

Muzhi Li[1, 2], Xingan Jiang[1]†, Zhuoyin Peng[2], Dongdong Zhang[1], Xue Chen[3], Xiangping Zhang[4], Xueyun Wang[5], Zhao Liang[1]† and Weiyou Yang[1]†

[1]*Institute of Micro/Nano Materials and Devices, Ningbo University of Technology, Ningbo, 315211, China*

[2]*School of Energy and Power Engineering, Changsha University of Science & Technology, Changsha, 410014, P. R. China*

[3]*Engineering Research Center for Semiconductor Integrated Technology, Institute of Semiconductors, Chinese Academy of Sciences, Beijing, 100083, China*

[4]*Department of Materials Science and Engineering, Southern University of Science and Technology, Shenzhen, Guangdong, 518055, P. R. China.*

[5]*School of Aerospace Engineering, Beijing Institute of Technology, Beijing, 100081, China*

Corresponding author: Jiangxa88@163.com; walleliang@hnu.edu.cn; weiyouyang@tsinghua.org.cn

The PDF file includes: Supplementary Figs. 1 to 15

Table of contents

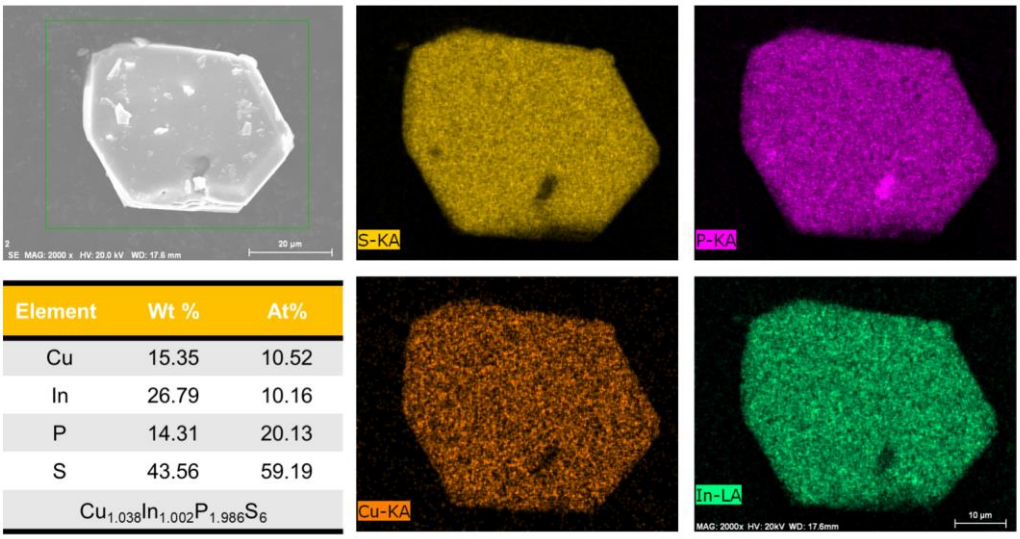

Element	Wt %	At%
Cu	15.35	10.52
In	26.79	10.16
P	14.31	20.13
S	43.56	59.19
$Cu_{1.038}In_{1.002}P_{1.986}S_6$		

Supplementary Fig. 1 | The composition of the as-grown crystals determined by energy dispersive X-ray spectroscopy. The stoichiometric ratio of Cu, In, P, and S elements is approximately 1:1:2:6.

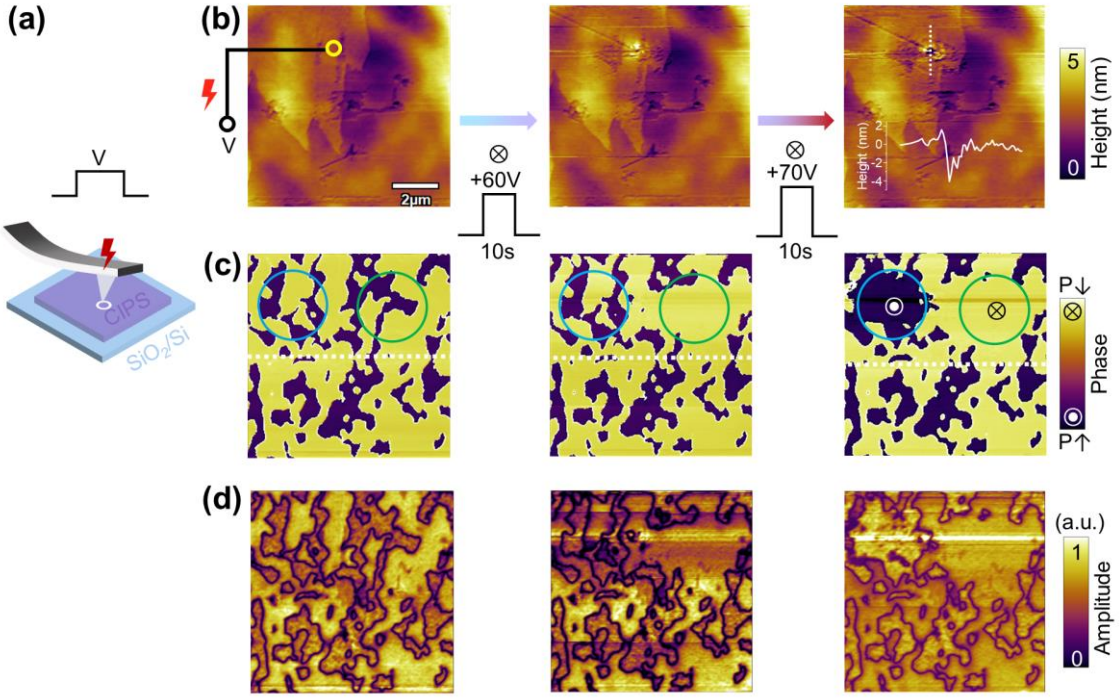

Supplementary Fig. 2 | Tip-bias application for minimal surface damage and efficient domain switching. **(a)** Schematic of the tip voltage application at a point location (yellow circle) under open-circuit conditions without current generation to prevent surface damage. **(b)** The topography before and after consecutive +60 V and +70 V pulses (10 s each), with minimal surface damage (local height change: 1–4 nm). **(c, d)** The as-measured ferroelectric domains (phase and amplitude) before and after bias application, where significant domain changes are indicated by the circles.

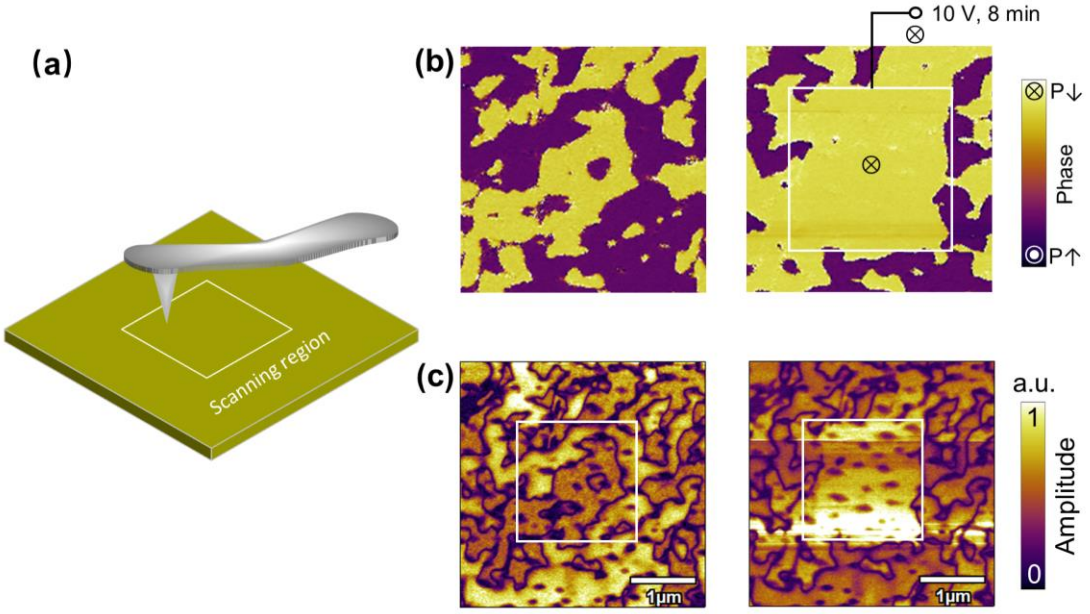

Supplementary Fig. 3 | Determination of polarization orientation for ferroelectric domains. (a) Schematic illustration of tip bias application to switch the ferroelectric domains over a scanning region. **(b-c)** The as-measured ferroelectric domains (phase and amplitude) before and after tip bias application. By applying a relatively small downward-pointing voltage (⊗, +10 V for 8 minutes), purple-black domains were switched to yellow domains, suggesting the downward polarization (⊗, $\boldsymbol{P}\downarrow$) in yellow domain regions and upward polarization (⦿, $\boldsymbol{P}\uparrow$) in purple-black domain regions.

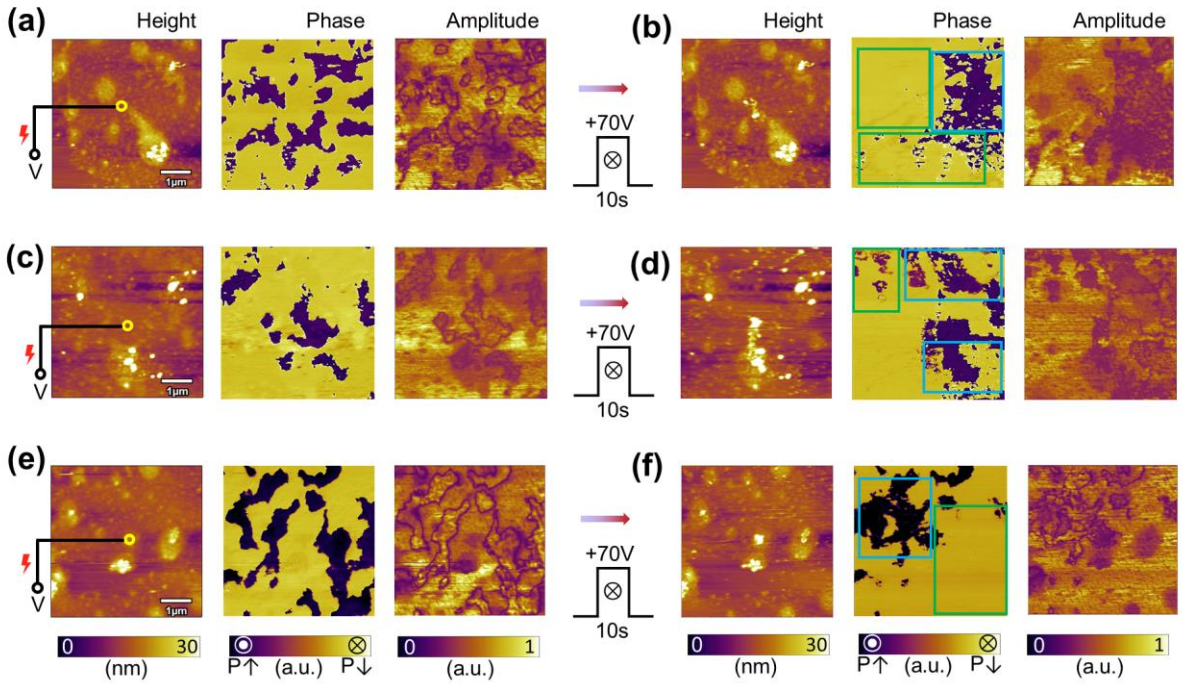

Supplementary Fig. 4 | The highly reproducible switching difference in spatial regions near the tip across multiple measurement locations. (a-f) The as-measured topography and ferroelectric domains (phase and amplitude) **(a, c, e)** before and **(b, d, f)** after bias application at three different regions. The downward-pointing voltage (⊗, +70 V for 10 s) was applied at the point location, as indicated by the yellow circle. In the green circled region, the purple-black domains (***P***↑) were switched to yellow domains (***P***↓). In the blue circled region, the yellow domains (***P***↓) were switched back to purple-black domains (***P***↑).

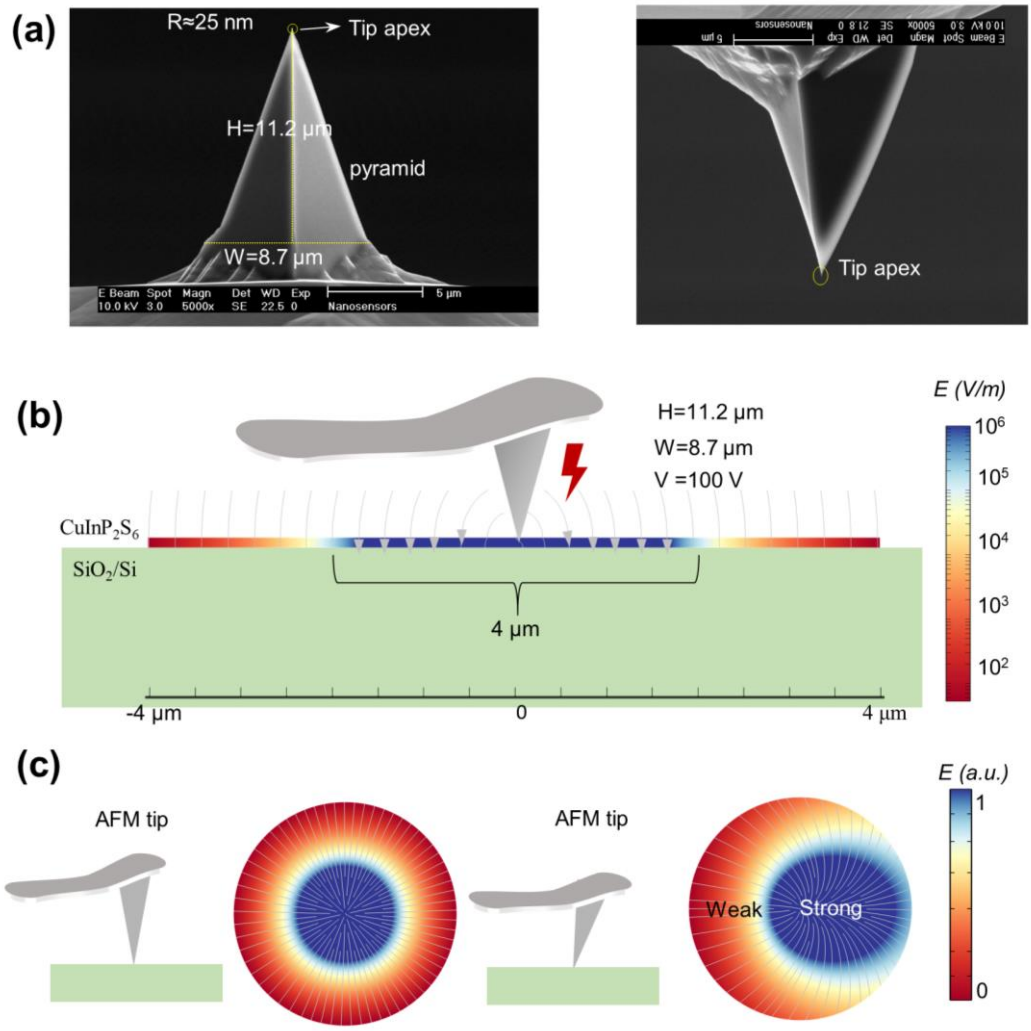

Supplementary Fig. 5 | The geometric shape of the scanning tip and electric field distribution. (**a**) The side view of a Pt/Ir coated AFM tip (Nanosensor PPP-EFM). The conductive tip has a representative pyramidal geometry with a height of ~11.2 μm, lateral dimensions of ~8.7 μm, and an apex radius of ~25 nm, respectively. Reproduced from NANOSENSORTm [https://www.nanosensors.com]. (**b**) The estimated electric field distribution based on a symmetry geometric shape of AFM tip. (**c**) The simulated tip electric field distribution. Asymmetry or slight tilting of the tip can significantly deviate this electric field from a symmetric, radially distributed electric field.

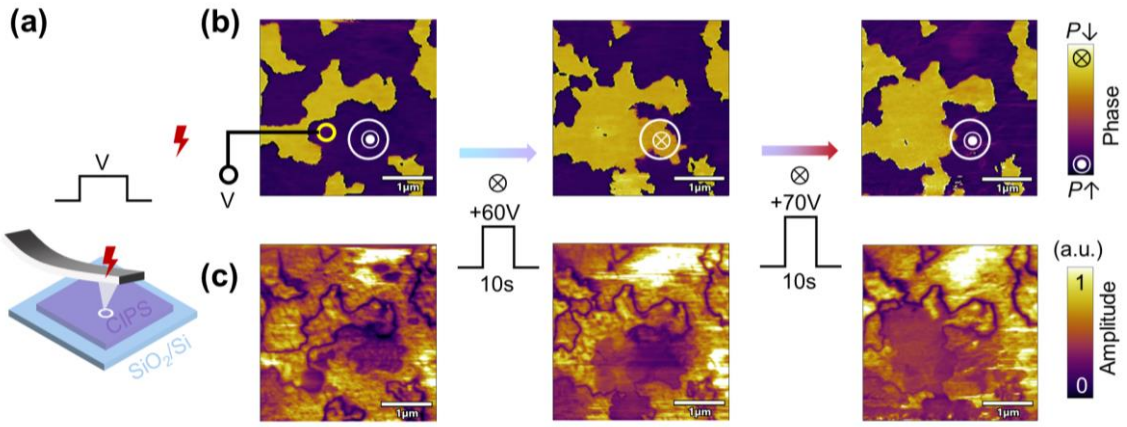

Supplementary Fig. 6 | Tip-bias application for minimal surface damage and cyclic domain switching at identical location. **(a)** Schematic of tip voltage application at a point location (yellow circle) under open-circuit conditions. **(b-c)** The as-measured ferroelectric domains (phase and amplitude) before and after consecutive +60 V and +70 V pulses (10 s each), with minimal surface damage (local height change: 1–4 nm).

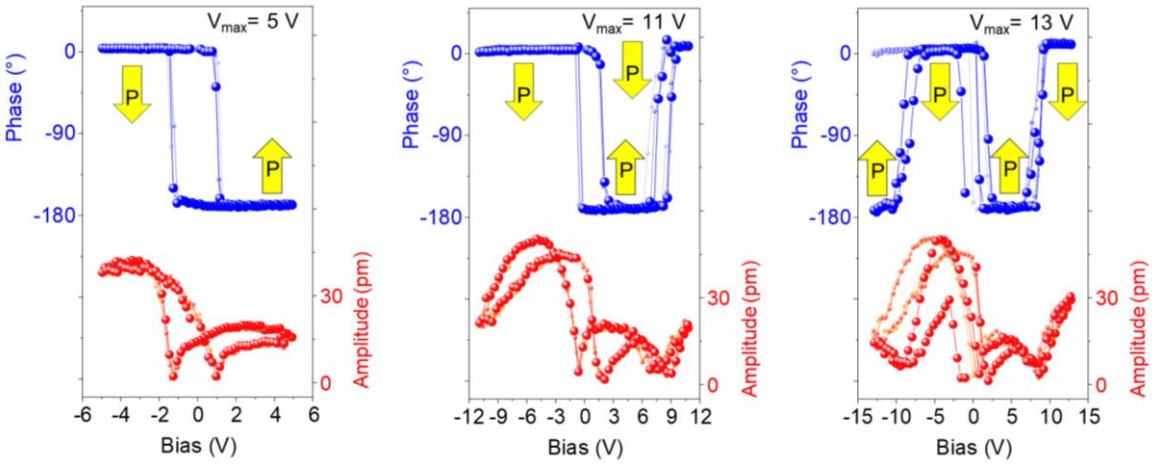

Supplementary Fig. 7 | The polarization switching within different bias window by switching spectroscopy PFM. Within V_{max} = 5 V, only one hysteresis loop was observed. The polarization aligns along the identical direction to external electric field. As the voltage window increased up to V_{max} = 11 V and V_{max} = 13 V, multiple hysteresis loops were observed. For example, with increasing positive bias magnitude, the polarization undergoes two consequent switching of $\boldsymbol{P}\downarrow \rightarrow \boldsymbol{P}\uparrow \rightarrow \boldsymbol{P}\downarrow$.

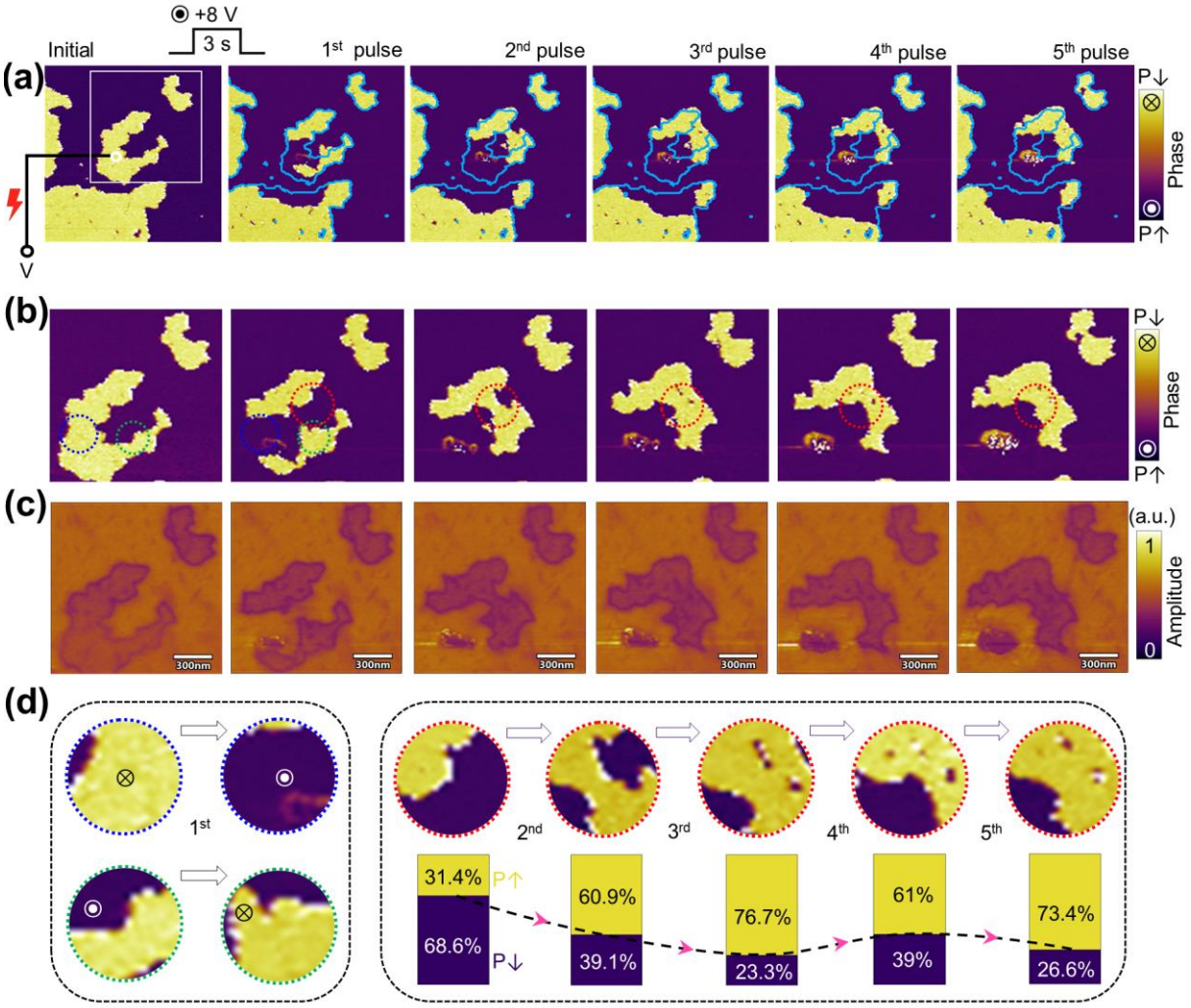

Supplementary Fig. 8 | The evolution of the ferroelectric domains under repeated bias application. (a) Ferroelectric domain evolution under five bias applications (+8V/3s). The location of voltage application was marked by white circle. The voltage was applied through the bottom conductive substrate. The region of pristine ferroelectric domains is highlighted with a blue outline. **(b-c)** The magnified view of the ferroelectric domain evolution after 1-5th bias application. Several regions with noticeable domain changes were marked with blue, green, and red circles. **(d)** The ferroelectric domain changes in the color circle region. After the 1st bias application, the ferroelectric domains were switched in opposite directions in the cyan and green circle regions. After the 2nd to 5th bias applications, the domains were switched in one direction, with alternating switching in the red circle region.

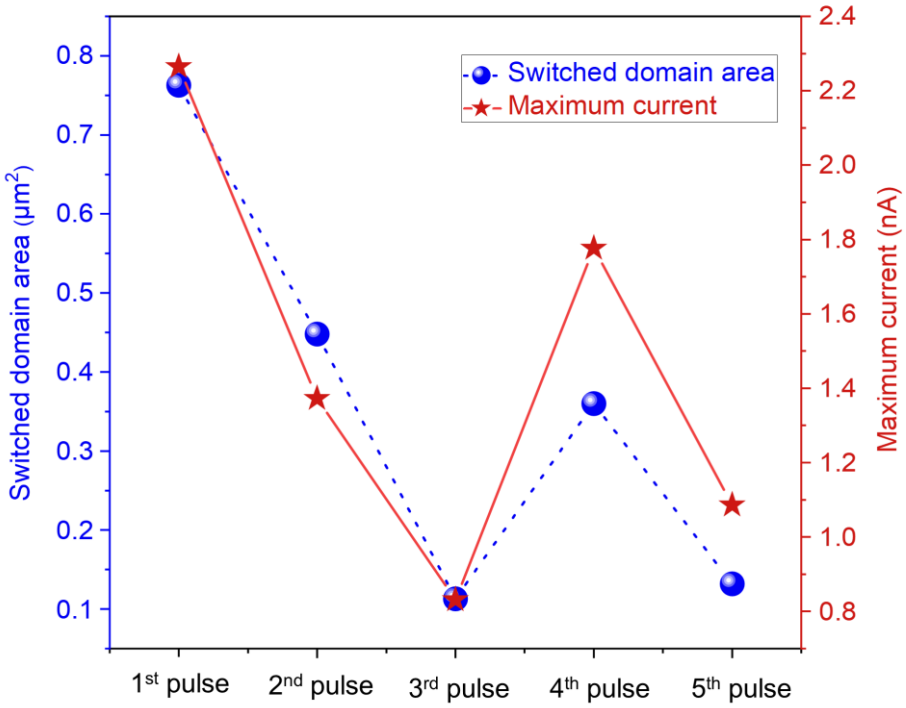

Supplementary Fig. 9 | The switched domain area and the measured maximum current for each voltage pulse based on the results in FIG. 2c in main text. The data clearly show that the current scales proportionally with the area of domain switching per voltage pulse.

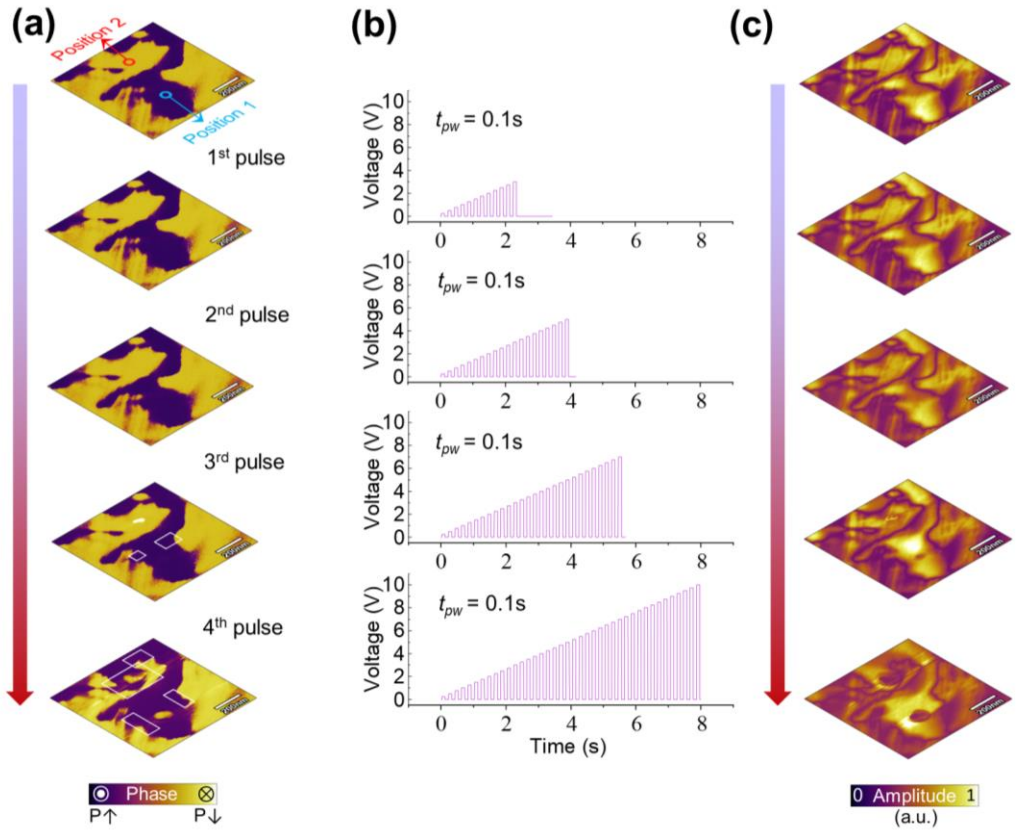

Supplementary Fig. 10 | The ferroelectric domain changes under varied voltage pulses. **(a, c)** The tracking of ferroelectric domain (phase and amplitude) changes. **(b)** The varied voltage pulses for four pulses.

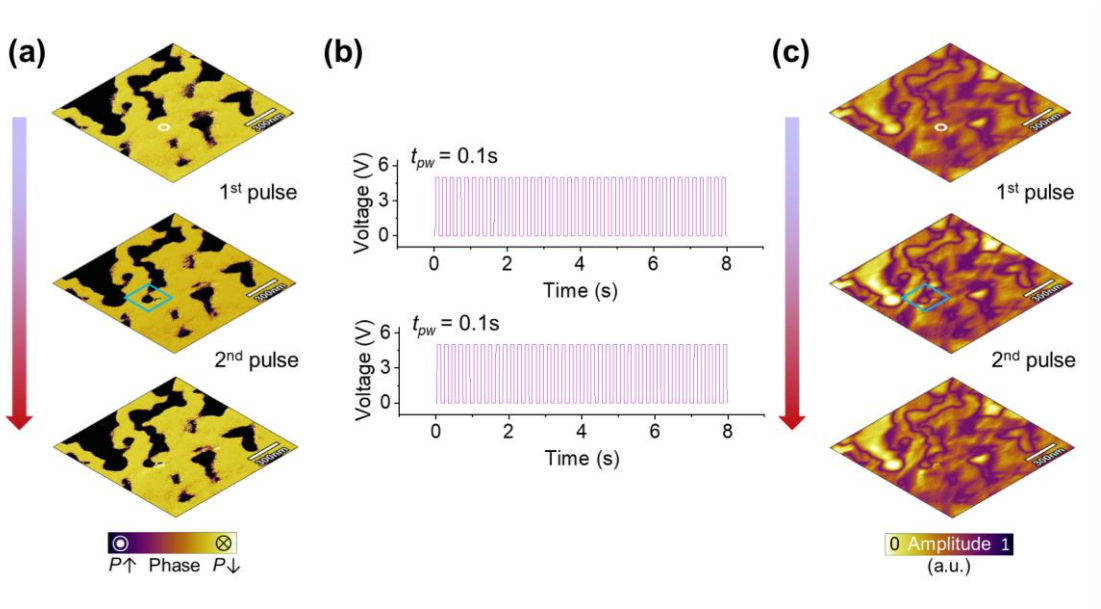

Supplementary Fig. 11 | The ferroelectric domain changes under continued voltage pulses. **(a, c)** The tracking of ferroelectric domain (phase and amplitude) changes. **(b)** The corresponding voltage pulses for two pulses.

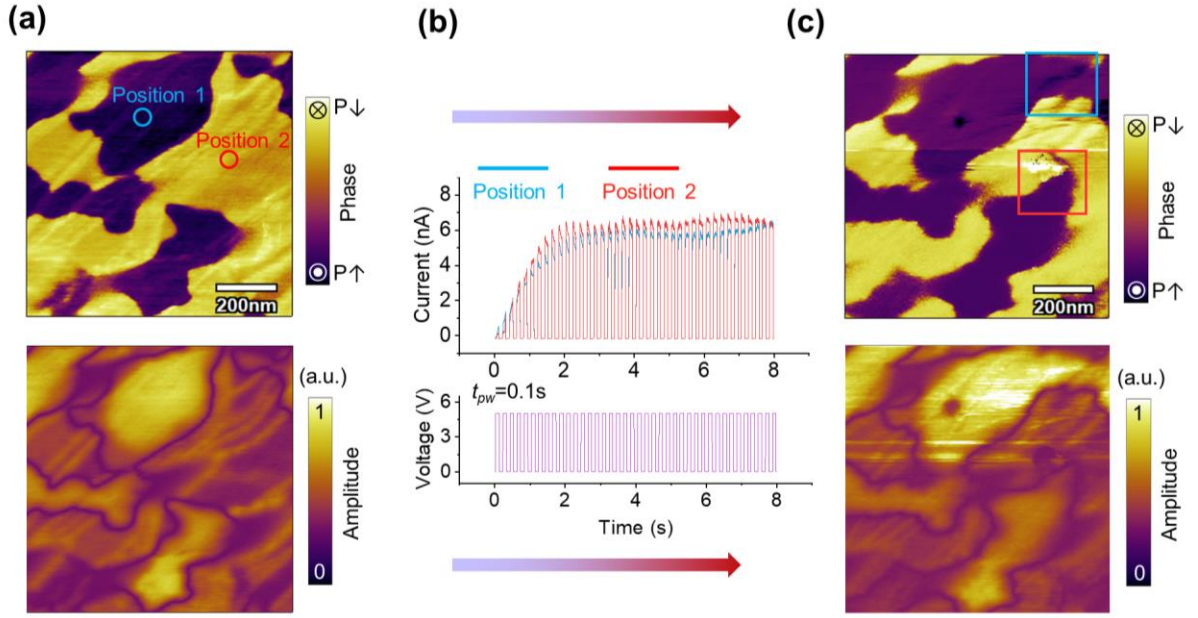

Supplementary Fig. 12 | Current response measured at oppositely-oriented ferroelectric domains. (a, c) The as-measured ferroelectric domain (phase and amplitude) evolution **(a)** before and **(c)** after bias application, with the tip positioned at oppositely-oriented ferroelectric domains. Pronounced polarization switching occurs in both regions, as indicated by blue and red boxes. **(b)** The applied voltage and the corresponding currents at two different locations. Identical voltage conditions at both positions yield nearly identical current magnitudes and responses.

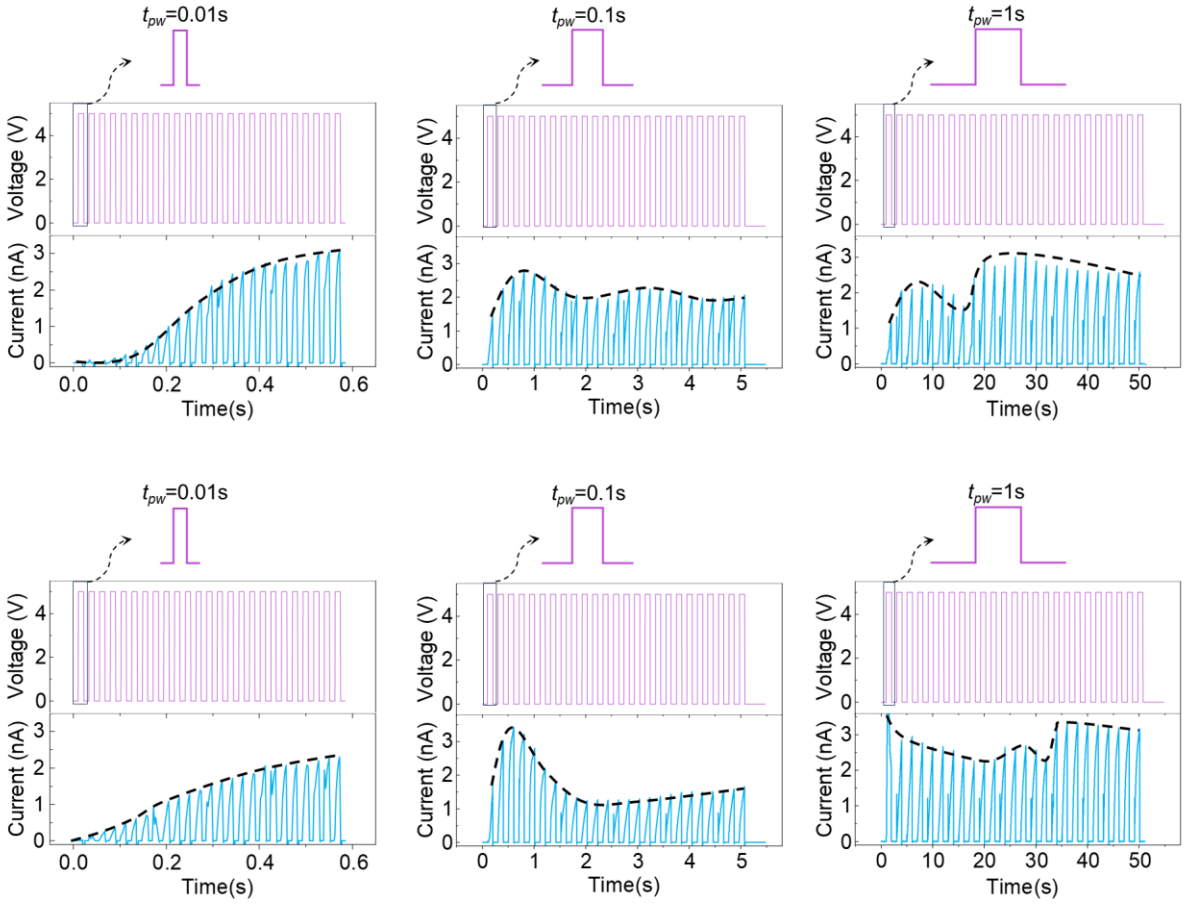

Supplementary Fig. 13 | Periodic current modulation via the varied pulse bias conditions across six adjacent point locations. The pulse voltage and number were maintained constant at 5 V and 25 cycles, respectively. Three sets of pulse widths (t_{pw} = 0.01 s, 0.1 s, and 1 s) were employed, demonstrating highly reproducible current modulation dependent on pulse widths.

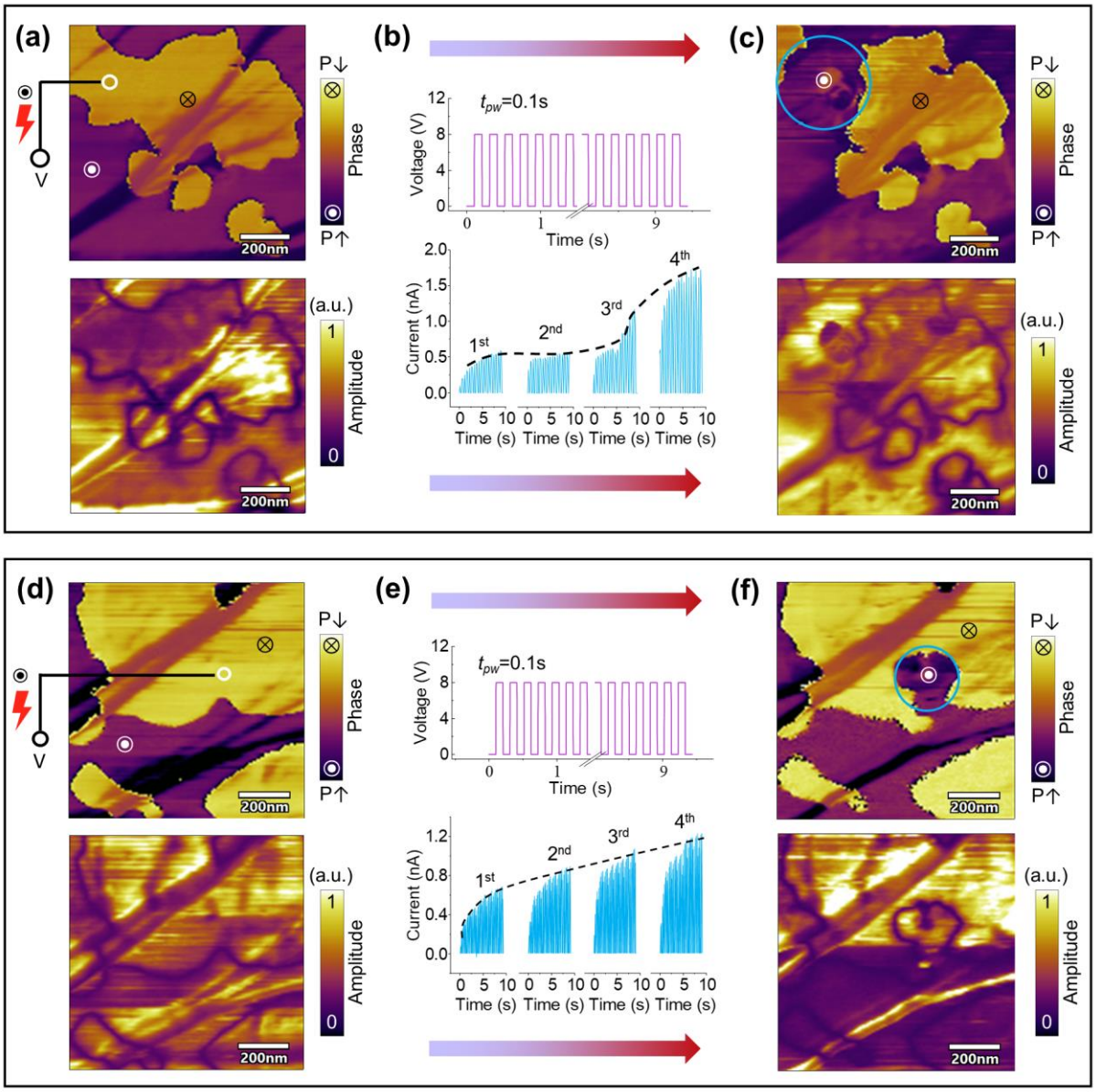

Supplementary Fig. 14 | The ferroelectric domain changes, together with the corresponding voltage pulses and current response at two different locations. (**a-f**) The ferroelectric domains (phase and amplitude) (**a, d**) before and (**c, f**) after (**b, e**) four pulse sets with the voltage (+8 V) and pulse width (t_{pw} = 0.1 s). Note that the current increases upon pulse stimulation, which agrees well with ferroelectric domain changes only beneath the AFM tip.

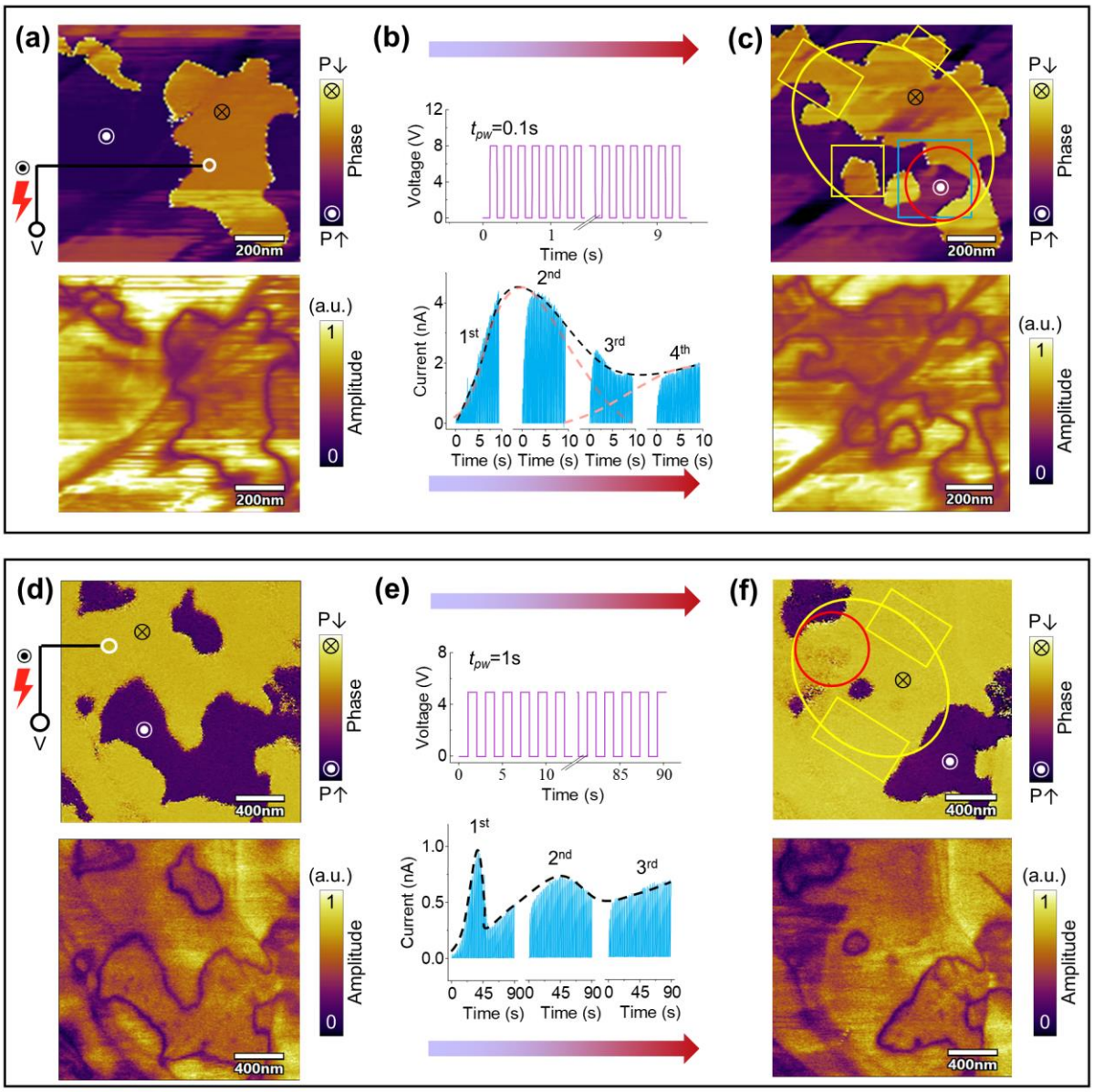

Supplementary Fig. 15 | The ferroelectric domain changes, together with the corresponding voltage pulses and current response at two different locations. (a-c) The ferroelectric domains (phase and amplitude) **(a)** before and **(c)** after **(b)** four pulse sets with the voltage (+8 V) and pulse width (t_{pw} = 0.1 s). **(d-f)** The ferroelectric domains (phase and amplitude) **(d)** before and **(f)** after **(e)** three pulse sets with the voltage (+5 V) and pulse width (t_{pw} = 1 s). Note that the ferroelectric domain changes occurs over broader areas and at different locations, which is consistent with multiple well-resolved current peaks.